Assessment of Cerebral Blood Flow Pulsatility and Cerebral Arterial Compliance With 4D Flow MRI

Madelene Holmgren, MS,[1*] Anders Wåhlin, PhD,[1,2] Tora Dunås, PhD,[1,2,3] Jan Malm, MD, PhD,[4] and Anders Eklund, PhD[1,2]

Background: Four-dimensional flow magnetic resonance imaging (4D flow MRI) enables efficient investigation of cerebral blood flow pulsatility in the cerebral arteries. This is important for exploring hemodynamic mechanisms behind vascular diseases associated with arterial pulsations.
Purpose: To investigate the feasibility of pulsatility assessments with 4D flow MRI, its agreement with reference two-dimensional phase-contrast MRI (2D PC-MRI) measurements, and to demonstrate how 4D flow MRI can be used to assess cerebral arterial compliance and cerebrovascular resistance in major cerebral arteries.
Study Type: Prospective.
Subjects: Thirty-five subjects (20 women, 79 ± 5 years, range 70–91 years).
Field Strength/Sequence: 4D flow MRI (PC-VIPR) and 2D PC-MRI acquired with a 3T scanner.
Assessment: Time-resolved flow was assessed in nine cerebral arteries. From the pulsatile flow waveform in each artery, amplitude (ΔQ), volume load (ΔV), and pulsatility index (PI) were calculated. To reduce high-frequency noise in the 4D flow MRI data, the flow waveforms were low-pass filtered. From the total cerebral blood flow, total PI (PI_{tot}), total volume load (ΔV_{tot}), cerebral arterial compliance (C), and cerebrovascular resistance (R) were calculated.
Statistical Tests: Two-tailed paired *t*-test, intraclass correlation (ICC).
Results: There was no difference in ΔQ between 4D flow MRI and the reference (0.00 ± 0.022 ml/s, mean ± SEM, $P = 0.97$, ICC = 0.95, $n = 310$) with a cutoff frequency of 1.9 Hz and 15 cut plane long arterial segments. For ΔV, the difference was –0.006 ± 0.003 ml (mean ± SEM, $P = 0.07$, ICC = 0.93, $n = 310$) without filtering. Total R was 11.4 ± 2.41 mmHg/(ml/s) (mean ± SD) and C was 0.021 ± 0.009 ml/mmHg (mean ± SD). ΔV_{tot} was 1.21 ± 0.29 ml (mean ± SD) with an ICC of 0.82 compared with the reference. PI_{tot} was 1.08 ± 0.21 (mean ± SD).
Data Conclusion: We successfully assessed 4D flow MRI cerebral arterial pulsatility, cerebral arterial compliance, and cerebrovascular resistance. Averaging of multiple cut planes and low-pass filtering was necessary to assess accurate peak-to-peak features in the flow rate waveforms.
Level of Evidence: 2
Technical Efficacy Stage: 2

J. MAGN. RESON. IMAGING 2020;51:1516–1525.

CARDIAC CONTRACTIONS generate pulsatile blood flow from the heart throughout the arterial tree. With age, stiffening of the elastic aortic wall causes a decrease in arterial compliance, resulting in increased pressure oscillations along the arterial tree.[1] Pulsatile load is suggested to increase the transmission of pulsations to the distal cerebral microcirculation[2,3] and hasten the progress of diseases such as cognitive impairment[4] and stroke.[5] An understanding of the interplay between arterial pulsatility and the development of vascular diseases is therefore important. For this purpose, three main circulatory mechanisms must be considered: First, the central aortic stiffening, which dictates the pulsatile load to the cerebral system; Second, the cerebral arterial compliance,

View this article online at wileyonlinelibrary.com. DOI: 10.1002/jmri.26978

Received Jul 16, 2019, Accepted for publication Oct 8, 2019.

*Address reprint requests to: M.H., Department of Radiation Sciences, Umeå University, 901 87 Umeå, Sweden. E-mail: madelene.holmgren@umu.se

From the [1]Department of Radiation Sciences, Umeå University, Umeå, Sweden; [2]Umeå Center for Functional Brain Imaging, Umeå University, Umeå, Sweden; [3]Center for Demographic and Aging Research, Umeå University, Umeå, Sweden; and [4]Department of Pharmacology and Clinical Neuroscience, Umeå University, Umeå, Sweden

which further dampen the pulsatility before it reaches the capillaries; and finally the cerebral vascular resistance, which affects the amount of pulsatile flow through the capillaries. Ideally, one would like to measure compliance and resistance directly, but this is difficult since suitable measurement techniques have been lacking and indirect pulsatility biomarkers, such as pulsatility index, are used as surrogates.

Cerebral blood flow and pulsations are traditionally measured with transcranial Doppler (TCD) ultrasonography[6] or two-dimensional phase-contrast magnetic resonance imaging (2D PC-MRI).[7,8] The TCD technique is limited by its need of a cranial window, and it does not provide flow rates in ml/s. 2D PC-MRI does not share that limitation but is time-consuming, since each artery is assessed separately. These limitations are resolved with the emerging technique of time-resolved 3D PC-MRI (4D flow MRI),[9] which provides a full coverage of the arterial tree in less than 10 minutes. Pulsatility measurements in cerebral arteries have previously been described with 4D flow MRI,[10,11] but remaining questions are how flow rate quantifications (beyond velocity) may unlock novel diagnostic measures and to what accuracy such measurements can be achieved.

Cerebral arterial pulsatility has been assessed using arterial pulsatile volume load (ΔV)[12–14] and pulsatility index (PI).[15,16] Additionally, cerebral arterial compliance (C) and cerebrovascular resistance (R), the two basic components in the two-element Windkessel model,[17] describe the functionality of the arterial system to dampen the pulsations.

In this study, the aim was to investigate the feasibility of pulsatility assessments with 4D flow MRI in cerebral arteries and its agreements with reference 2D PC-MRI measurements for flow waveform amplitudes (ΔQ), ΔV and PI. The aim was also to demonstrate how 4D flow MRI can be utilized for the analysis of cerebral arterial compliance and cerebrovascular resistance.

Materials and Methods

Subjects

Forty-one participants from a previously studied cohort, with subjects recruited in 2007,[18] were invited for a new physical examination and MRI in the fall of 2017. Of the invited participants, 37 underwent the MRI. Of these, two subjects were not included in the analysis due to incomplete image acquisitions. The final study population was 35 elderly subjects (20 women, 79 ± 5 years, range 70–91 years). At a physical examination, carried out on a separate occasion from the MRI, blood pressure was noninvasively measured in the left arm, risk factors and diseases were noted, and the current health status was examined by a neurologist. These characteristics are presented in Table 1, along with heart rate during the MRI. Noted risk factors were hypertension (n = 23), hyperlipidemia (n = 14), current smoking (n = 1), and previous smoking (n = 6). Diseases were atrial fibrillation (n = 3), diabetes mellitus (n = 2), ischemic heart disease (n = 2), and cerebrovascular disease (n = 2). Additionally, two subjects had Alzheimer's disease.

TABLE 1. Blood Pressure Characteristics of the Included Subjects

(N = 35)	Mean ± SD
SBP (mmHg)	144 ± 17
DBP (mmHg)	87 ± 10
PP (mmHg)	57 ± 15
MAP (mmHg)	106 ± 11
HR (bpm)	66 ± 10

N, number of subjects; SD, standard deviation; SBP, systolic blood pressure; DBP, diastolic blood pressure; PP, pulse pressure (SBP-DBP); MAP, mean arterial pressure approximated as DBP + (1/3) PP; HR, heart rate (during the magnetic resonance imaging).

To calculate cerebrovascular resistance and cerebral arterial compliance, each subject's specific intracranial pressure (ICP) recorded at the previous study of this cohort[18] was used. In four subjects, no ICP was obtained, and in these cases, the median reference value from the original cohort was used. The median ICP for this study was 11.6 mmHg. No new measurements or age adjustments of the ICP values were performed. Except from the use of ICP values, there was no relationship with respect to the purpose between the previous and the current study.

The study was approved by the local Ethical Review Board. Written informed consent was obtained from all participants.

MRI

The scan protocol was previously described.[19] It included 4D flow MRI followed by multiple 2D PC-MRI acquisitions, without any contrast agent, performed on a 3T scanner (GE Discovery MR 750, Milwaukee, WI) with a 32-channel head coil. The 4D flow MRI sequence was a balanced 5-point[20] phase contrast vastly undersampled isotropic projection reconstruction (PC-VIPR)[9] sequence with full brain coverage (repetition time / echo time [TR/TE] 6.5/2.7 msec, Venc 110 cm/s, flip angle 8°, 16,000 radial projections, acquisition resolution 300 × 300 × 300, imaging volume 22 × 22 × 22 cm^3, reconstructed resolution 320 × 320 × 320, zero padded interpolation, isotropic voxel size 0.7 × 0.7 × 0.7 mm^3, 20 reconstructed cardiac time-frames). The Venc was a three-directional velocity encoding scheme that utilizes five encoding points.[20] The scan time was about 9 minutes. A T_1-weighted magnitude image, an angiographic complex difference image (CD) (Fig. 1), and velocity images in three directions were reconstructed. Eddy current correction of the 4D flow MRI data was performed in the reconstruction.

Measurement planes perpendicular to nine cerebral arteries (Fig. 1) were covered in eight 2D PC-MRI acquisitions (TR/TE 7.6–10.7/4.1–4.7 msec, Venc 60–100 cm/s, flip angle 15°, in-plane resolution 0.35 × 0.35 mm^2, slice thickness 3 mm, matrix size 512 × 512 voxels, 32 time-resolved images reconstructed). The scan time for each acquisition was about 3 minutes. The measured arteries were the left (L) and right (R) internal carotid arteries (ICA), covered in one plane just below the skull base, the basilar artery (BA), the L

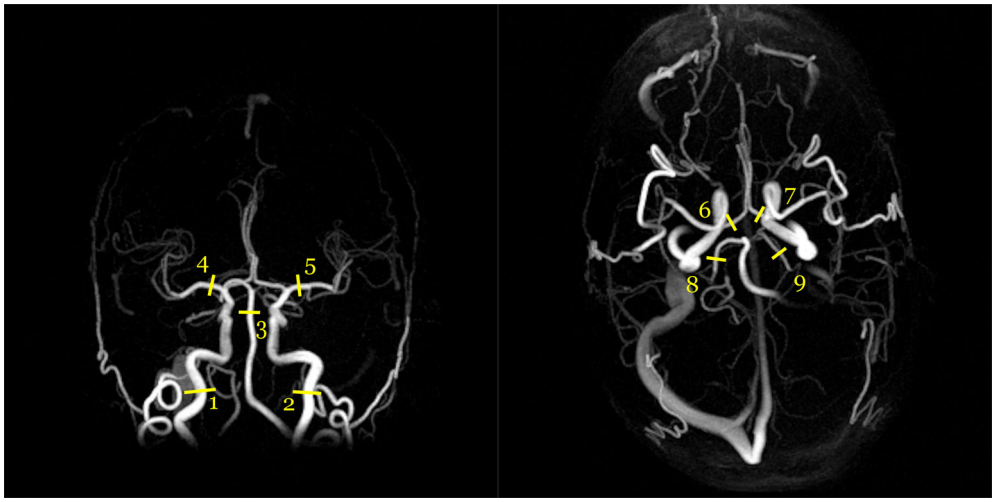

FIGURE 1: Angiographic maximum intensity projections of a complex difference image (CD) for one subject from the coronal view (left) and the axial view (right). The coronal projection is from a subset of the image. The numbers indicate approximate center points of the measurement sites at (1, 2) the ICAs, (3) the BA, (4, 5) the MCAs, (6, 7) the ACAs, and (8, 9) the PCAs.

and R middle cerebral arteries (MCA) at the M1 level, the L and R anterior cerebral arteries (ACA) at A1 level, and the L and R posterior cerebral arteries (PCA) at P2 level. When the first branch of the MCA bifurcated immediately, as it did for two arteries, the two distal branches were covered in one plane and the flow in them was summed in the postprocessing.

2D PC-MRI Segmentation

Segmentation and eddy current correction of the 2D PC-MRI data were processed using the software Segment v2.1 R5960 (http://medviso.com).[21] A region of interest (ROI) covering each artery was manually outlined, considering both the magnitude and the phase image. The ROI was kept constant through all time frames. Inter-rater reliability for these segmentations has previously been shown to be excellent.[19]

Processing of 4D Flow MRI Data

A centerline representation of the vascular tree was used to locate the correct arterial branch in the brain volume.[11,22] The centerline representation was based on a binary image, created by thresholding the CD volume to remove background signals.[11] This image was gradually thinned to a one-voxel-thick centerline.[23,24] To avoid a mismatch in spatial location between the 4D flow MRI and 2D PC-MRI datasets, the center coordinate of each segmented ROI in the 2D PC-MRI plane was transformed to the corresponding location in the 4D flow MRI data.[19] The centerline voxel closest to the located coordinate was used as the seed point in the segmentation method. All seed points were visually inspected, and manually adjusted in case of mismatch.[19]

Segmentation Method for 4D Flow MRI

In this study, a previously introduced methodology[19] for segmentation, based on local thresholding, was used for quantification of blood flow rates in cerebral arteries. Cut planes were extracted from the CD volume and resampled in the direction of the arteries, perpendicular to the velocity direction of the arterial flow, using the centerline representation of the branches. Fifteen cut planes, if possible, around each seed point were extracted, compared to one cut plane in the previous study. Each cut plane had a thickness of one voxel, and a size of 17×17 voxels in the plane, extracted from the region around the centerline voxel. Before vessel segmentation, the voxels in the planes were linearly interpolated by a factor of four. Thresholding was performed on each cut plane separately, where the threshold was chosen as 16% of the maximum intensity in the plane. The 16% threshold used for time-resolved reconstructed 4D flow MRI data was selected since it produced a mean flow corresponding to the reference 2D PC-MRI data. The threshold was slightly lower than the 20% threshold established for mean flow reconstruction.[19] A binary ROI of the segmented artery was thus generated, from which the flow within the ROI was summed, keeping the same ROI size for each of the 20 cardiac phases. Each segmentation was visually inspected and manually corrected if necessary. Manual correction was necessary in 22% of the cut planes, almost exclusively in ACA and PCA.

Multiple Cut Planes and Low-Pass Filtering

Different noise levels were found in the flow waveforms when comparing 2D PC-MRI with 4D flow MRI. Due to the largely undersampled 4D flow MRI sequence, a lower signal-to-noise ratio (SNR), compared to the 2D PC-MRI reference, was expected. To account for this potential problem, we investigated how averaging of multiple cut planes and low-pass filtering of the 4D flow MRI waveforms could reduce the high-frequency noise. Flow waveforms from one to 15 consecutive cut planes along the centerline, each with a thickness of 0.7 mm, were averaged to evaluate the potential noise reduction of the blood flow waveforms. The 15 cut planes could be acquired in almost all arteries, where the length of the unbranched MCA was the primary limitation. In these cases, the available cut planes where used instead. Each waveform was low-pass filtered with cutoff frequencies ranging from 1–4 Hz, in steps of 0.1 Hz. Before filtering, each waveform was repeated 30 times to elongate the signal. Only the center filtered waveform was used for analysis.

Pulsatility Measures

MEAN, SYSTOLIC, AND DIASTOLIC BLOOD FLOW. The mean flow rate (Q_{mean}), the systolic (Q_{syst}), and the diastolic (Q_{dias}) peaks of the flow waveforms were determined. The flow peak-to-peak pulsatility amplitude ΔQ was calculated as the difference between the systolic and the diastolic flow, $\Delta Q = Q_{syst} - Q_{dias}$.

ARTERIAL PULSATILE VOLUME LOAD. Due to compliance, the arterial walls distend in response to cardiac-induced pressure variations. The blood volume accumulated in the artery will therefore vary over the cardiac cycle. In addition, there is a pulsatile flow through the capillaries. These two pulsatile components form the flow waveform and will represent the accumulated pulsatile volume load (ΔV) to the arterial tree distal to a measurement point. ΔV is assessed by subtracting Q_{mean} from the flow waveform (Q) and cumulatively integrate:

$$\Delta V = \int_{Systole} (Q(t) - Q_{mean})\, dt \tag{1}$$

where systole is defined as the part where $Q(t) - Q_{mean} > 0$.[13] An approximation of the total pulsatile volume load (ΔV_{tot}) of the cerebral arterial system during one cardiac cycle was obtained by summing the waveforms for the left and right ICA and BA.[12,25] Arterial-specific ΔV calculated for MCA, ACA, or PCA also gives a possibility to analyze the regional contribution to the cerebral arterial compliance from the different cerebral arterial territories.

RELATIONSHIP BETWEEN ΔQ AND ΔV. By approximating the flow waveforms to be represented as sinusoidal functions, it can be shown that ΔQ and ΔV are related by:

$$\Delta Q = \omega \Delta V \tag{2}$$

where ω expresses the heart rate (HR) as $\omega = 2\pi HR/60$ (HR in bpm). Thus, peak-to-peak waveform ΔQ and the integrated waveform ΔV are closely related by heart rate.

CEREBRAL ARTERIAL COMPLIANCE AND CEREBROVASCULAR RESISTANCE. Compared to cerebrovascular pulsatility measurements (ΔQ and ΔV), the resistance and compliance of the arteries indicate how the pulsations are managed in the arteries. It will be shown how ΔQ (or $\omega \Delta V$) can be used as input to assess the compliance. The cerebral arterial tree can be modeled as a two-element Windkessel model,[17] where a resistance term (R) represents the total cerebrovascular resistance and a compliance term (C_{WK}) represents the capacity of the arteries to accumulate blood.

The total impedance (Z) of the Windkessel model can, with the electrical analogy, be expressed as:

$$|Z| = \frac{R}{\sqrt{1 + \omega^2 R^2 C_{WK}{}^2}} \tag{3}$$

and shows the dependency of R and C. The cerebrovascular impedance at frequency equal to heart rate can be approximated as:

$$Z = \frac{PP}{\Delta Q} \tag{4}$$

where PP is the pulse pressure amplitude of the blood pressure.[26] The cerebrovascular resistance is:

$$R = \frac{MAP - ICP}{Q_{mean}} \tag{5}$$

where MAP is the mean arterial pressure and ICP is the intracranial pressure. Using Eqs. 4 and 5 in Eq. 3, and solving for C_{WK} at heart rate, the cerebral arterial compliance for the two-element Windkessel model can be deduced as:

$$C_{WK} = \frac{\sqrt{\left(\frac{(MAP-ICP)}{PP}\frac{\Delta Q}{Q_{mean}}\right)^2 - 1}}{\left(\frac{\omega\,(MAP-ICP)}{Q_{mean}}\right)} \tag{6}$$

This two-element impedance-based approach, according to Eq. 6, is the main compliance model in this study. However, we will compare it to a simplified model where a nonpulsatile flow at the terminal arteries is assumed, requiring the assumption of a completely dampened pulse pressure, thus leaving all pulsations to the compliant arteries. With that simplification, compliance is calculated as the ratio between the volume load and the pressure change[25] (C_{VP}) expressed as:

$$C_{VP} = \frac{\Delta V}{PP} \tag{7}$$

which thus is an approximation of the cerebral arterial compliance.

PULSATILITY INDEX. A popular way to describe pulsations in arteries is by calculating Gosling's pulsatility index (PI) from the flow waveform of the arteries.[15] The corresponding PI for blood flow rates was calculated by dividing the amplitude of the flow waveform by the mean flow:

$$PI = \frac{\Delta Q}{Q_{mean}} \tag{8}$$

PI from flow rates should be the same as for velocity assessments with ultrasound if a laminar parabolic blood flow velocity profile in the measured artery is assumed. Using Eqs. 5 and 8 in Eq. 6, and solving for PI, gives:

$$PI = \frac{PP}{MAP - ICP}\sqrt{(\omega RC)^2 + 1} \tag{9}$$

Revealing PI as a composite index including the product of C and R.[26]

Statistical Analysis

The 4D flow MRI pulsatility measurements were evaluated by comparing ΔQ and ΔV with the corresponding 2D PC-MRI values. All differences were calculated as 2D – 4D. To evaluate the effects of filtering, the chosen cutoff frequency was the one resulting in the lowest absolute mean difference of ΔQ between 4D flow MRI and 2D PC-MRI. PI and ΔV from 4D flow MRI were also evaluated against 2D PC-MRI for the separate arteries. The mean differences between 4D flow MRI and 2D PC-MRI are presented as mean ± standard error of mean (SEM). Other mean values are mean ± standard deviation (SD). Two-tailed paired *t*-tests were used to test for all differences between 4D flow MRI and 2D PC-MRI. For all tests, the significance level was set at $P < 0.05$. Intraclass correlation, $ICC_{(2,1)}$, was used to investigate correlations.[27] Bland–Altman plots were used to visualize the agreement between methods. MatLab R2019a (MathWorks, Natick, MA) was used for all postprocessing and statistical analysis.

Results

Pulsatile Amplitude and Volume Load

A total of 310 arteries were available for evaluation. There was no difference in mean flow rate between 4D flow MRI and 2D PC-MRI measurements (–0.009 ± 0.014 ml/s, $P = 0.52$). First, the need for noise reduction of the flow pulsatility measurements, ΔQ and ΔV, was examined. For ΔQ, the agreement between 4D flow MRI and the reference, as a function of the number of cut planes and cutoff frequencies of the low-pass filter, is illustrated in Fig. 2a,b. At all frequencies, the highest ICC was consistently found for 15 cut planes, with no difference at the cutoff frequency 1.9 Hz (0.00 ± 0.022 ml/s, $P = 0.97$), yielding an ICC of 0.95 (Fig. 3a,c). As a comparison, without filtering, the mean difference was –0.285 ± 0.024 ml/s ($P < 0.001$) with an ICC of 0.92, revealing the need for filtering. Figure 4 shows the effect of filtering on the right MCA waveforms, for each of the 35 subjects, with the reference waveforms as a comparison. Regarding ΔV, 15 cut planes again showed the highest ICC. Unfiltered data showed no difference between 4D flow MRI and the reference (–0.006 ± 0.003 ml, $P = 0.07$) and an ICC of 0.93 (Fig. 3b,d). No correlation in the difference between methods with respect to the age of the subjects was found for ΔQ ($r = –0.10$, $P = 0.07$) or ΔV ($r = –0.07$, $P = 0.22$). Accordingly, the subsequent analysis was based on 15 cut planes of 4D flow MRI data, and for ΔQ filtered with a 1.9 Hz cutoff frequency, while ΔV was calculated from unfiltered 4D flow MRI data.

For total cerebral pulsatile volume load, ΔV_{tot}, there was an ICC of 0.82 between 4D flow MRI and the reference (Fig. 5a,b), with a 4D mean ΔV_{tot} of 1.21 ± 0.29 ml ($n = 34$). Total cerebral arterial PI, calculated by Eq. 8 and the summed flow in the two ICA and BA, was $PI_{tot} = 1.08 \pm 0.21$ ($n = 34$). For all arteries, the ICC for PI was 0.58 between 4D flow MRI and the reference.

Theoretically, ΔQ and ωΔV should be equal if sinusoidal flow and pressure waveforms are assumed (Eq. 2). Indeed, there was an excellent agreement (ICC of 0.97) between ΔQ and ωΔV ($n = 310$) (Fig. 6), but ωΔV was lower, with a mean difference of 0.175 ± 0.211 ml/s ($P < 0.001$), likely reflecting a deviation from a perfect sinusoidal waveform.

Cerebral Arterial Compliance and Resistance

Using ΔQ, Q_{mean} and HR of 4D flow MRI waveforms together with measured subject-specific PP, MAP, and ICP, Eqs. 5 and 6 were used to assess cerebrovascular resistance and cerebral arterial compliance, with all data available in 33 subjects. The total cerebrovascular resistance

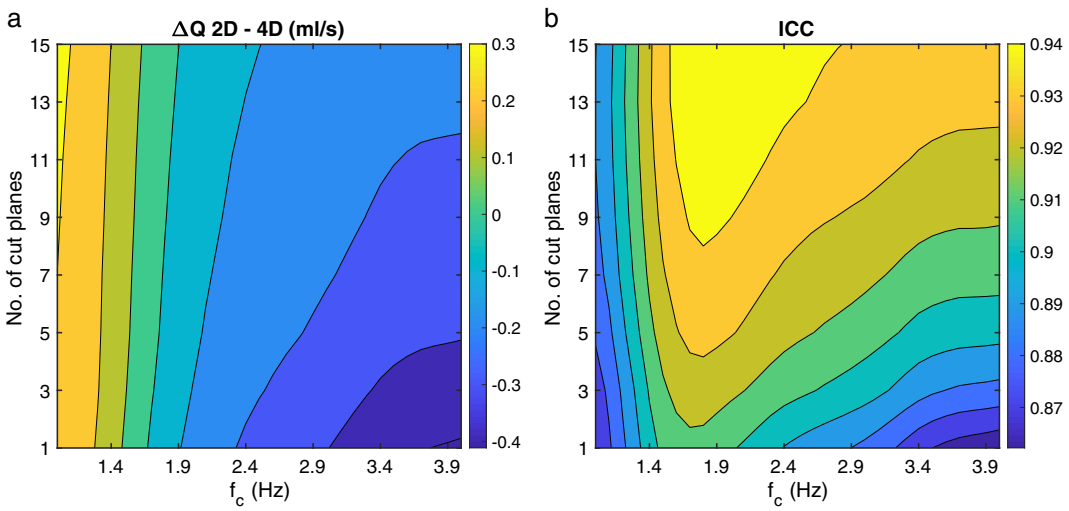

FIGURE 2: (a) Mean difference (ml/s) of flow peak-to-peak waveform amplitudes (ΔQ), and (b) ICC between 2D PC-MRI and 4D flow MRI, for the range of cutoff frequencies (f_c) of the low-pass filter (horizontal axis) and the number of cut planes (vertical axis). The color bar to the right of each figure shows the magnitude of the mean difference and the ICC, respectively.

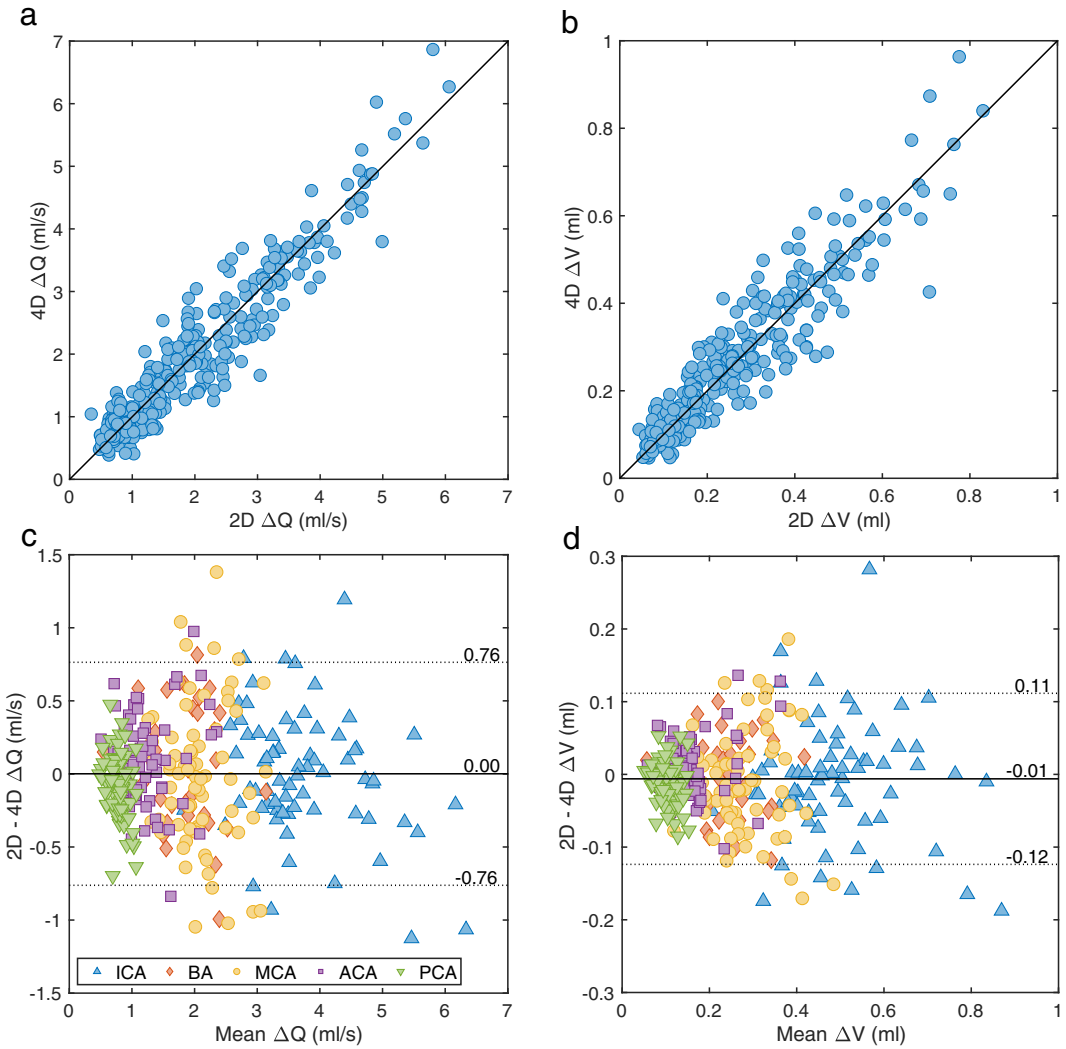

FIGURE 3: Correlation plots for (a) flow peak-to-peak waveform amplitude (ΔQ) and (b) ΔV between 2D PC-MRI and 4D flow MRI for all arteries (n = 310) with ICCs of 0.95 and 0.93, respectively. The solid line represents the line of equality. (c) Bland–Altman analysis of the agreement between methods for ΔQ and (d) for ΔV, where the solid line represents the mean difference and dotted lines are the 95% confidence intervals.

was R = 11.4 ± 2.41 mmHg/(ml/s) (n = 33) and the total cerebral arterial compliance was C_{WK} = 0.021 ± 0.009 ml/mmHg (n = 33).

The simplified model, assuming a nonpulsatile capillary flow, C_{VP}, according to Eq. 7 with ΔV_{tot} as input, showed an excellent agreement against C_{WK} (ICC of 0.94) but with a

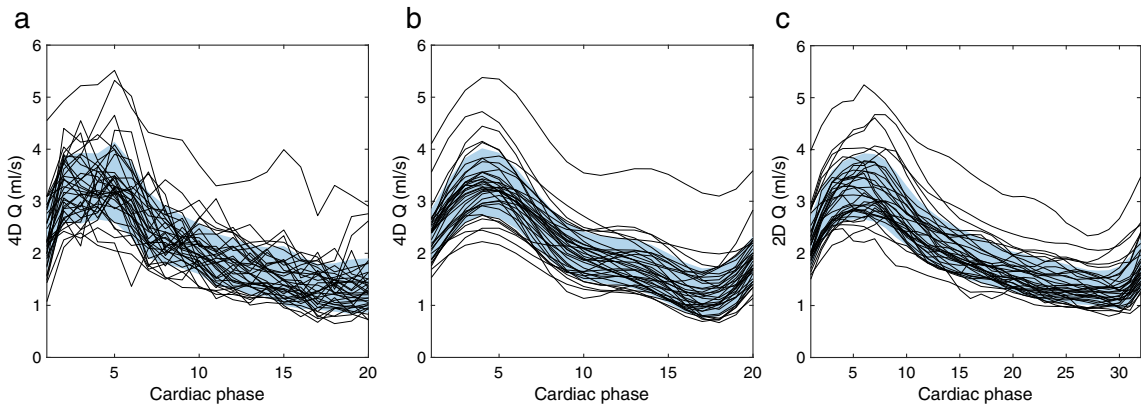

FIGURE 4: Flow rate waveform of the right MCA for each of the 35 subjects. (a) Unfiltered and (b) filtered waveforms from 4D flow MRI data and (c) reference waveforms from 2D PC-MRI data. The blue region is the mean value in each cardiac phase, with ±1 SD in width.

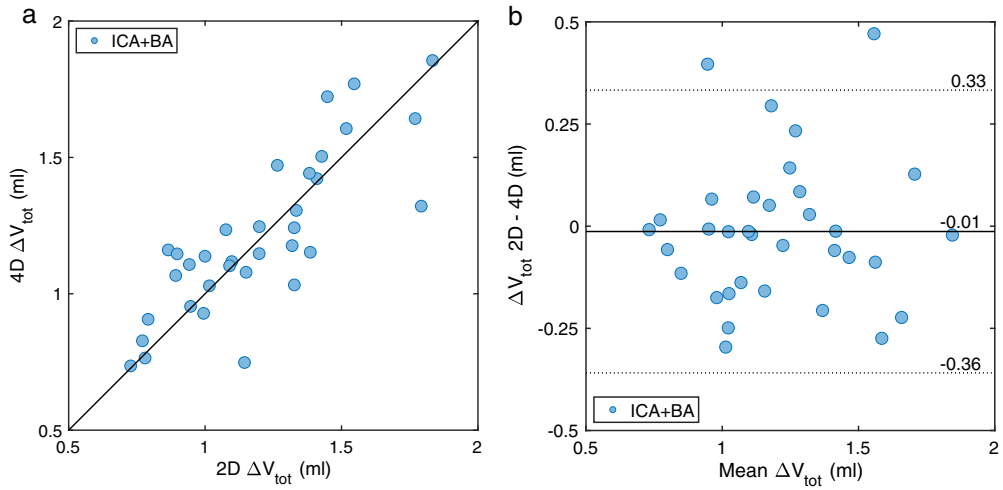

FIGURE 5: The combined ΔV of the left and right ICAs and the BA, for 2D PC-MRI compared with the unfiltered 4D flow MRI data. (a) Correlation between methods, with an ICC of 0.82 (n = 34). The solid line represents the line of equality. (b) Bland–Altman analysis of the agreement between methods. The solid line represents the mean difference and dotted lines are the 95% confidence intervals.

higher estimated compliance ($P < 0.001$), with an average difference of 11% (Fig. 7).

Pulsatility in Separate Arteries

For studying the separate arteries, Table 2 shows the mean for PI and ΔV, and the ICC between 4D flow MRI and the reference. In general, they showed a good concordance for the large arteries, ICA, BA, and MCA, while for the smaller arteries, ACA and PCA, there was a limited agreement, particularly for PI.

Discussion

The feasibility of 4D flow MRI for quantifying cerebrovascular compliance, resistance, and pulsatility was investigated. An excellent concordance with reference 2D PC-MRI was found for ΔV and ΔQ. For ΔQ, the 4D flow MRI data first had to be denoised. We show how cerebral arterial compliance and cerebral vascular resistance can be assessed using the 4D flow MRI and blood pressure data.

An elevated pulsatile load is suggested to impact the progress of diseases such as cognitive impairment[4] and

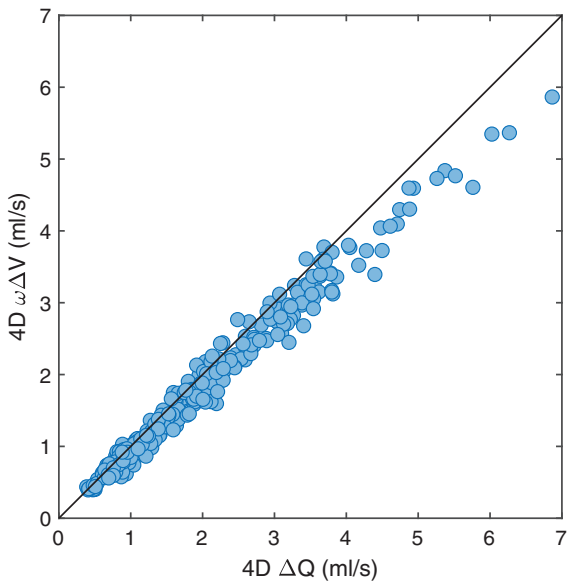

FIGURE 6: Correlation between the ΔQ and the corresponding ωΔV for the arterial waveforms measured with 4D flow MRI for all arteries (n = 310). The frequency (ω) was related to heart rate (HR) by ω = 2πHR/60. The ICC was 0.97. The solid line represents the line of equality.

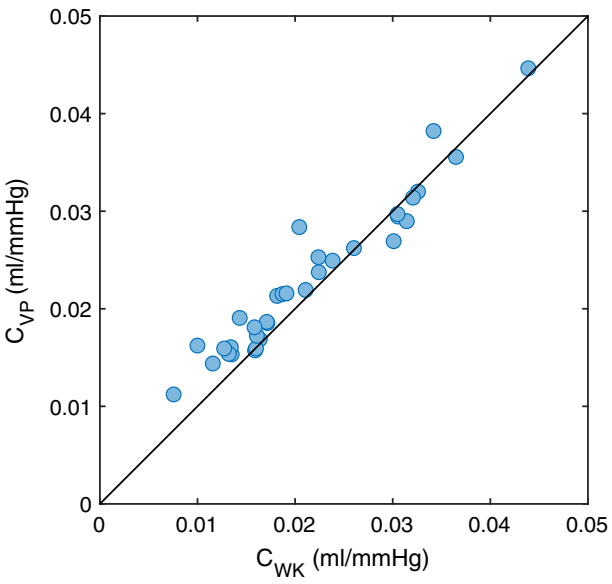

FIGURE 7: Correlation between the two expressions for cerebral arterial compliance (C_{WK} and C_{VP}) with a difference in assumption about peripheral pulsatility (n = 33), based on the combined waveforms of the left and right ICAs and the BA. The ICC was 0.94. The solid line represents the line of equality. The overestimation was most pronounced at low compliant arteries.

TABLE 2. Mean and ICC of 4D Flow MRI and Reference 2D PC-MRI for Different Arteries

			PI (mean ± SD)		ΔV (ml) (mean ± SD)		
Artery	**N**	**4D (1.9 Hz)**	**2D**	**ICC**	**4D**	**2D**	**ICC**
ICA	70	1.10 ± 0.23	1.10 ± 0.20	0.84	0.49 ± 0.14	0.48 ± 0.14	0.83
BA	34	1.03 ± 0.24	1.04 ± 0.20	0.59	0.24 ± 0.08	0.24 ± 0.08	0.76
MCA	70	1.02 ± 0.25	1.00 ± 0.20	0.63	0.28 ± 0.08	0.27 ± 0.08	0.62
ACA	67	0.93 ± 0.26*	1.02 ± 0.23	0.49	0.16 ± 0.06	0.16 ± 0.07	0.78
PCA	69	1.02 ± 0.28*	0.94 ± 0.15	0.37	0.11 ± 0.03**	0.10 ± 0.02	0.39

4D flow MRI, four-dimensional flow magnetic resonance imaging; 2D PC-MRI, two-dimensional phase-contrast magnetic resonance imaging; ICC, intraclass correlation; PI, pulsatility index; ΔV, volume load (ml); SD, standard deviation; ICA, internal carotid artery; BA, basilar artery; MCA, middle cerebral artery; ACA, anterior cerebral artery; PCA, posterior cerebral artery.
*Significant difference ($P < 0.05$).
**Significant difference ($P < 0.001$).

stroke,[5] where the pulsatile load is characterized by an elevated pulsatile blood flow and pulse pressure.[28] The effect increases with the age-related stiffening of the arterial walls,[29] where the decreased compliance increases the aortic pulse pressure.[30] All parts of the arterial tree contribute to the total arterial compliance, but it is believed that the primary contribution comes from the distension of the large central arteries, like the aorta.[3,29] Thus, from a cerebral perspective we have to consider the pulsatile input that the central circulation provides to the cerebral circulation, which is mainly due to the heart output and the central arterial compliance, but we also have to consider the ability of the cerebral arterial compliance to further dampen the pulsatility before it reaches the capillaries.

This study shows that when cerebral artery flow rate waveforms from MRI are available, the analysis of cerebral pulsatility can be extended beyond the composite biomarkers such as PI. The pulsatile input to the cerebral system is generated by PP, which produces a total volumetric pulsatile load to the cerebral system, characterized by ΔQ and ΔV. These are dependent and dampened by the patient-specific properties of the cerebral arterial compliance, C, and the cerebrovascular resistance, R. All of these measures can be estimated using 4D flow MRI combined with pressure data.

To quantify cerebral arterial compliance from ΔQ or ΔV, we implemented the well-established two-element Windkessel model of cerebrovascular hemodynamics and deduced an expression (Eq. 6) which, in addition to ΔQ and Q_{mean} from 4D flow MRI, required MAP, PP, and an ICP. Thus, we demonstrated a method for individual assessment of the cerebral arterial tree's contribution to vascular compliance, and with that, an approximation of the dampening capacity of the cerebral arteries. In this demonstration we utilized 10-year-old measurements of ICP. However, on a group level, no change in mean ICP is expected over this time period,[31] and a sensitivity analysis revealed a variation of about 1% in C_{WK} when assuming an ICP variability within 1 SD. Based on that, we believe that the estimated C_{WK} should be representative for C_{WK} of an elderly population. Furthermore, if a pathological ICP disturbance is not expected in an investigated subject, the assumption of an ICP of about 11 mmHg is probably sufficient for a reliable assessment of C_{WK}, thus avoiding the need for ICP measurements.

The general concordance between the two approaches of assessing compliance, C_{WK} and C_{VP}, was high, with a small overestimation of the volume-pressure model for the lower range of compliances. In the two-element Windkessel model, a decreased compliance means that the relative pulsatile flow in the resistance part increases, ie, pulsatile flow through the capillaries, since the impedance of the compliance element increases. Therefore, in the simplified model, an overestimation is expected for lower compliances, in agreement with our results. Thus, the two-element Windkessel model better accounts for the relationship between the cerebral arterial compliance and the resistance.

When comparing 4D and 2D flow MRI sequences, there is a trade-off between whole-brain coverage and temporal resolution with higher SNR levels. We found that denoising through multiple cut planes and low-pass filtering of the flow rate waveform were necessary to obtain enough SNR to detect the systolic and diastolic blood flow peaks, ie, ΔQ, in concordance with the high-resolution 2D PC-MRI data. With a sufficiently large number of voxels used to assess an average arterial waveform, the signal gets more reliable. This was accomplished by using the maximum of 15 cut planes. For vessels with diameters on the size of ACA, PCA, or smaller, we recommend using as many cut planes as possible to reduce noise and improve flow assessment accuracy.

It should be noted that both C and R can be calculated from 2D PC-MRI waveforms. The advantage of 4D flow MRI is the simultaneous flow acquisition and avoidance of the preselection of the measurement planes. For quantification of total cerebral C and R, the methods are comparable, since only one 2D PC-MRI plane is required to determine total cerebral blood flow and pulsatility.

As a measure based on the entire waveform, rather that peak-to-peak range, ΔV was less sensitive than ΔQ to high-frequency noise and showed a good agreement on a group level and for the separate arteries even without the low-pass filtering. The total arterial pulsatile volume load was lower than previously reported results.[12,25,32] This difference may be explained by the high age of this cohort, thus leading to a lower expected inflow and a lower cerebral vascular compliance. Besides an analysis of the total volume load from the total cerebral inflow, 4D flow MRI acquisitions also offer a unique possibility for regional analysis of arterial pulsatile volume load as input to the vascular territories of MCA, ACA, and PCA. The correlation between methods in our study was in agreement with a previously published pilot study from our research group.[13] These measurements of ΔV can then be utilized in terms of regional compliance analysis by using the approach of Eq. 6 for each arterial territory.

PI is an established parameter for analysis of pulsations in the cerebrovascular arteries.[33] Historically, this is because the self-normalizing ratio design suits ultrasound velocity measurements in MCA. The PI values found in this study, both for 2D and 4D, were in the same range, or slightly higher, as those determined in a previous 2D PC-MRI[16] and in a large TCD study.[33] The difference is possibly explained by the higher mean age, since there is a documented age dependency.[33] Since PI is directly based on the ΔQ measurements (Eq. 8), 15 cut planes and low-pass filtered flow waveforms are recommended to obtain a reliable PI from 4D flow MRI. Compared to a previous 4D study with PC-VIPR,[10] our PI estimates were lower. This is natural, since we have introduced low-pass filtering to improve the SNR, which affects the PI estimation.

As shown in Eq. 9, PI is a composite measurement of pulsatility,[26] and therefore has limitations in the analysis of the specific compensatory capacity (R and C) of the arterial system. To fully understand the dynamics of pulsations in relation to, for example, arterial stiffening, the R and C should be analyzed in addition to PI.

In a previous study on these data, with the aim to automize vessel segmentation and flow rate assessment, a reduced concordance between methods for PCA measurements was observed.[19] A major change in the current study was therefore to manually correct segmentations in cut planes where the local thresholding method could not isolate the artery of interest in the segmentation. This was to prioritize the accuracy and quality of estimated blood flow rate waveforms, at the expense of the automatization of the workflow for flow rate segmentation with 4D flow MRI. Additionally, the 4D flow MRI data were reconstructed into time-resolved frames, unlike the previous study. This caused a small but significant change in the mean flow rates in the arteries. This change forced us to decrease the threshold level in the segmentation, to maintain a nonsignificant mean flow rate difference.

A limitation of the present analysis is that the flow rates and blood pressure were not simultaneously investigated. Further, blood pressure was not measured at the same anatomical site as the flow rate assessment. This limits our possibilities for an accurate pressure and flow phase shift analysis, along with a difference between the cerebral and the brachiocephalic pulse pressure.[34] We have presented a method to estimate arterial compliance, and that accuracy can be improved by noninvasive blood pressure measurements performed simultaneously inside the MR scanner.[35] The two-element Windkessel model is a basic approximation, where three- and four elements have extended the model to better represent the full flow waveform. However, for pulsatility measurements related to the heart cycle, the two-element still provides a good approximation for a basic compliance estimation with 4D flow MRI.[17]

In conclusion, time-resolved 4D flow MRI data were accurate for pulsatility analysis in large cerebral arteries, but the reduced SNR level required postprocessing, such as low-pass filtering and multiple cut plane averaging, to reliably detect peak-to-peak features in the waveforms. With the post-processing requirement included, we demonstrate the feasibility of 4D flow MRI assessment of cerebral arterial pulsatility, cerebral arterial compliance, and cerebrovascular resistance. These measurements offer a comprehensive description of the cerebral circulatory system, which has the potential to advance our understanding of the interplay between arterial pulsatility and the development of cerebral vascular diseases.

Acknowledgment

Contract grant sponsor: Swedish Research Council; Contract grant number: 2015–05616 (to A.E.); Contract grant sponsor: County Council of Västerbotten (to A.E.); Contract grant sponsor: Swedish Heart and Lung Foundation; Contract grant number: 20140592 (to J.M.); Contract grant sponsor: County Council of Västerbotten (to J.M.); Contract grant sponsor: Swedish Research Council; Contract grant number: 2017-04949 (to A.W.); Contract grant sponsor: County Council of Västerbotten (to A.W.).

The authors thank research nurse Kristin Nyman for skillful work with the volunteer subjects.

References

1. London GM, Pannier B. Arterial functions: How to interpret the complex physiology. Nephrol Dial Transplant 2010;25:3815–3823.
2. Wåhlin A, Nyberg L. At the heart of cognitive functioning in aging. Trends Cogn Sci 2019:1–3.
3. Mitchell GF. Effects of central arterial aging on the structure and function of the peripheral vasculature: Implications for end-organ damage. J Appl Physiol 2008;105:1652–1660.
4. Mitchell GF, van Buchem MA, Sigurdsson S, et al. Arterial stiffness, pressure and flow pulsatility and brain structure and function: The Age, Gene/Environment Susceptibility-Reykjavik Study. Brain 2011;134: 3398–3407.
5. Chuang S-Y, Cheng H-M, Bai C-H, Yeh W-T, Chen J-R, Pan W-H. Blood pressure, carotid flow pulsatility, and the risk of stroke. Stroke 2016;47: 2262–2268.
6. Lim E-Y, Yang D-W, Cho A-H, Shim YS. Cerebrovascular hemodynamics on transcranial Doppler ultrasonography and cognitive decline in mild cognitive impairment. J Alzheimers Dis 2018;65:651–657.
7. Zarrinkoob L, Ambarki K, Wåhlin A, Birgander R, Eklund A, Malm J. Blood flow distribution in cerebral arteries. J Cereb Blood Flow Metab 2015;35:648–654.
8. Zhao M, Amin-Hanjani S, Ruland S, Curcio AP, Ostergren L, Charbel FT. Regional cerebral blood flow using quantitative MR angiography. AJNR Am J Neuroradiol 2007;28:1470–1473.
9. Gu T, Korosec FR, Block WF, et al. PC VIPR: A high-speed 3D phase-contrast method for flow quantification and high-resolution angiography. AJNR Am J Neuroradiol 2005;26:743–749.
10. Rivera-Rivera LA, Turski P, Johnson KM, et al. 4D flow MRI for intracranial hemodynamics assessment in Alzheimer's disease. J Cereb Blood Flow Metab 2016;36:1718–1730.
11. Schrauben E, Ambarki K, Spaak E, Malm J, Wieben O, Eklund A. Fast 4D flow MRI intracranial segmentation and quantification in tortuous arteries. J Magn Reson Imaging 2015;42:1458–1464.
12. Wåhlin A, Ambarki K, Hauksson J, Birgander R, Malm J, Eklund A. Phase contrast MRI quantification of pulsatile volumes of brain arteries, veins, and cerebrospinal fluids compartments: Repeatability and physiological interactions. J Magn Reson Imaging 2012;35:1055–1062.
13. Wåhlin A, Ambarki K, Birgander R, et al. Measuring pulsatile flow in cerebral arteries using 4D phase-contrast MR imaging. AJNR Am J Neuroradiol 2013;34:1740–1745.
14. Ambarki K, Hallberg P, Jóhannesson G, et al. Blood flow of ophthalmic artery in healthy individuals determined by phase-contrast magnetic resonance imaging. Investig Ophthalmol Vis Sci 2013;54:2738–2745.
15. Gosling RG, King DH. Arterial assessment by Doppler-shift ultrasound. J R Soc Med 1974;67:447–449.
16. Zarrinkoob L, Ambarki K, Wåhlin A, et al. Aging alters the dampening of pulsatile blood flow in cerebral arteries. J Cereb Blood Flow Metab 2016;36:1519–1527.
17. Westerhof N, Lankhaar J-W, Westerhof BE. The arterial Windkessel. Med Biol Eng Comput 2009;47:131–141.
18. Malm J, Jacobsson J, Birgander R, Eklund A. Reference values for CSF outflow resistance and intracranial pressure in healthy elderly. Neurology 2011;76:903–909.
19. Dunås T, Holmgren M, Wåhlin A, Malm J, Eklund A. Accuracy of blood flow assessment in cerebral arteries with 4D flow MRI: Evaluation with three segmentation methods. J Magn Reson Imaging 2019;50: 511–518.
20. Johnson KM, Markl M. Improved SNR in phase contrast velocimetry with five-point balanced flow encoding. Magn Reson Med 2010;63: 349–355.
21. Heiberg E, Sjögren J, Ugander M, Carlsson M, Engblom H, Arheden H. Design and validation of Segment — Freely available software for cardiovascular image analysis. BMC Med Imaging 2010;10:1–13.
22. Dunås T, Wåhlin A, Ambarki K, Zarrinkoob L, Malm J, Eklund A. A stereotactic probabilistic atlas for the major cerebral arteries. Neuroinformatics 2017;15:101–110.
23. Palágyi K, Kuba A. A 3D 6-subiteration thinning algorithm for extracting medial lines. Pattern Recognit Lett 1998;19:613–627.
24. Chen Z, Molloi S. Automatic 3D vascular tree construction in CT angiography. Comput Med Imaging Graph 2003;27:469–479.
25. Bateman GA, Levi CR, Schofield P, Wang Y, Lovett EC. Quantitative measurement of cerebral haemodynamics in early vascular dementia and Alzheimer's disease. J Clin Neurosci 2006;13:563–568.
26. De Riva N, Budohoski KP, Smielewski P, et al. Transcranial Doppler pulsatility index: What it is and what it isn't. Neurocrit Care 2012;17: 58–66.
27. Koo TK, Li MY. A guideline of selecting and reporting intraclass correlation coefficients for reliability research. J Chiropr Med 2016;15: 155–163.
28. Tarumi T, Ayaz Khan M, Liu J, et al. Cerebral hemodynamics in normal aging: Central artery stiffness, wave reflection, and pressure pulsatility. J Cereb Blood Flow Metab 2014;34:971–978.
29. Avolio AP, Chen SG, Wang RP, Zhang CL, Li MF, O'Rourke MF. Effects of aging on changing arterial compliance and left ventricular load in a northern Chinese urban community. Circulation 1983;68:50–58.
30. Belz GG. Elastic properties and windkessel function of the human aorta. Cardiovasc Drugs Ther 1995;9:73–83.
31. Fleischman D, Berdahl JP, Zaydlarova J, Stinnett S, Fautsch MP, Allingham RR. Cerebrospinal fluid pressure decreases with older age. PLoS One 2012;7:1–9.
32. Wåhlin A, Ambarki K, Birgander R, Malm J, Eklund A. Intracranial pulsatility is associated with regional brain volume in elderly individuals. Neurobiol Aging 2014;35:365–372.
33. Tegeler CH, Crutchfield K, Katsnelson M, et al. Transcranial Doppler velocities in a large, healthy population. J Neuroimaging 2013;23: 466–472.
34. Izzo JL. Brachial vs. central systolic pressure and pulse wave transmission indicators: A critical analysis. Am J Hypertens 2014;27:1433–1442.
35. Whittaker JR, Driver ID, Venzi M, Bright MG, Murphy K. Cerebral autoregulation evidenced by synchronized low frequency oscillations in blood pressure and resting-state fMRI. Front Neurosci 2019;13:1–12.